Available online at www.sciencedirect.com
SCIENCE DIRECT
Journal of Solid State Chemistry 179 (2006) 1762–1767
JOURNAL OF SOLID STATE CHEMISTRY
www.elsevier.com/locate/jssc

Crystal structure and high-pressure properties of γ-Mo_2N determined by neutron powder diffraction and X-ray diffraction

Craig L. Bull[a,b,*], Tetsuya Kawashima[c,d], Paul F. McMillan[c,e,*], Denis Machon[e], Olga Shebanova[e], Dominik Daisenberger[c], Emmanuel Soignard[f], E. Takayama-Muromachi[d], Laurent C. Chapon[b]

[a]*SUPA, School of Physics and Centre for Science at Extreme Conditions, University of Edinburgh, Mayfield Road, Edinburgh EH9 3JZ, UK*
[b]*ISIS Facility, Rutherford Appleton Laboratory, Chilton, Didcot, OX11 0QX, UK*
[c]*Davy Faraday Research Laboratory, The Royal Institution of Great Britain, 21 Albemarle Street, WBX 4BS, London, UK*
[d]*Superconducting Materials Centre (Namiki-site), National Institute for Materials Science (NIMS) 1-1 Namiki, Tsukuba Ibaraki, 305-0044 Japan*
[e]*Department of Chemistry and Materials Chemistry Centre, Christopher Ingold Laboratory, University College London, 20 Gordon Street, WC1H 0AJ, London, UK*
[f]*Department of Geological Sciences, Arizona State University, US*

Received 31 August 2005; received in revised form 31 January 2006; accepted 15 March 2006
Available online 19 April 2006

Abstract

We prepared samples of cubic γ-MoN_x ($x\sim0.5$) by high-pressure–high-temperature synthesis. N atom site occupancies within the defect rock salt structure were determined from time-of-flight neutron diffraction and powder X-ray diffraction data by Rietveld analysis. The results show that N atoms occupy only octahedral sites within the structure. The semi-metallic compound is a superconductor, with $T_c = 5.2$ K determined by SQUID magnetometry. The compressibility of the material was determined by synchrotron X-ray diffraction measurements at high pressure in the diamond anvil cell. The vibrational density of states was studied by Raman scattering spectroscopy.

Keywords: High pressure; Raman spectroscopy

1. Introduction

Refractory transition metal nitrides possess technologically important properties including high hardness and superconductivity [1–5]. Within the Mo–N system, known phases include the stoichiometric hexagonal compound δ-MoN and the non-stoichiometric cubic phase γ-MoN_x, with $x\sim0.5$ (γ-Mo_2N) [1,4]. δ-MoN is a high-hardness material with very low compressibility [6]. It is also a superconductor, with T_c values ranging between 12 and 15 K, depending upon the preparation conditions and degree of structural order [7–9]. The cubic $B1$-structured phase prepared by conventional methods has a stoichiometry near $MoN_{0.5}$ (i.e., Mo_2N). It is also superconducting, with $T_c = 4-5$ K [5]. The corresponding stoichiometric cubic nitride NbN has $T_c = 17$ K [1,5]. It was predicted that if stoichiometric cubic "γ-MoN" could be synthesized, it could achieve T_c values as high as 29 K [10]. However, ab initio theoretical predictions and recent high-P,T synthesis experiments have indicated that a fully nitrided cubic phase is unlikely to be achieved in the Mo–N system [11,12].

Within $B1$-structured nitrides, one *fcc* lattice is defined by the transition metal atoms, and the N atoms are presumed to occupy interstitial octahedral sites to form the second interpenetrating *fcc* lattice. Vacancies on the anion sublattice result in non-stoichiometric nitrides such as $MoN_{0.5}$, VN_x and TiN_x. However, although the N atoms are usually modelled as occupying only octahedral

*Corresponding authors. Davy Faraday Laboratory, School of Physics and Centre for Science at Extreme Conditions, University of Edinburgh, Mayfield Road, Edinburgh EH9 3JZ, UK. Fax: +44 1235 445720.
E-mail addresses: c.bull@rl.ac.uk (C.L. Bull), p.f.mcmillan@ucl.ac.uk (P.F. McMillan).

0022-4596/$ - see front matter © 2006 Elsevier Inc. All rights reserved.
doi:10.1016/j.jssc.2006.03.011

positions, their relative size indicates that they could also occupy tetrahedral sites within the structure, especially among heavy transition metal nitrides [1]. Neutron diffraction is ideally suited to study the N atom positions and site occupancy because of the large scattering length for nitrogen compared with the metal atoms (the bound coherent scattering cross sections of Mo and N are 5.7 and 11.01 barns, respectively). Here we have used neutron diffraction data for a sample of Mo_2N prepared by high-pressure syntheses [9,13]. The data were of sufficient quality for Rietveld refinement allowing the determination of nitrogen site occupation. We also studied the material by X-ray powder diffraction, and determined the compressibility by in situ angle-dispersive synchrotron X-ray diffraction measurements in the diamond anvil cell. We studied the vibrational density of states (vDOS) by Raman scattering spectroscopy.

2. Experimental methods

The starting material for synthesis experiments was a commercial γ-Mo_2N powder obtained from High Purity Chemicals, Japan (99.99%). High-pressure–high-temperature treatments were carried out to obtain phase-pure Mo_2N using a flat-belt-type high-pressure apparatus at the National Institute for Materials Science (NIMS), Japan, at 7.7 GPa and at 1673 K for 1 h. A total of 300 mg of the commercially obtained material was sealed in a gold capsule for the high-P,T experiments. There was no observable weight loss ($<0.1\%$ weight difference before and after each run), indicating that no nitrogen leaked from the capsules during the runs.

Recovered samples were characterised by X-ray powder diffraction using a Philips-PW1800 diffractometer and CuK_α radiation. Structural parameters were refined from the data via the Rietveld method using the programme RIETAN-2000 [14]. The space group $Fm\bar{3}m$ was assumed for γ-Mo_2N, and the occupation of the Mo site was fixed at 1.0. All major peaks in the powder X-ray pattern were successfully indexed by this model and were included in the refinement, except for four weak peaks due to an unknown impurity (2θ values 35.6–36.4°, 41.4–41.8°, 60.1–60.5°, 71.9–72.4°). The 1 1 1 and 2 0 0 peaks were refined using a split pseudo-Voigt function. The refined lattice parameter and N site occupancy are reported in Table 1, and the result of the Rietveld fit to the X-ray data is shown in Fig. 1(a).

Time-of-flight (TOF) neutron diffraction experiments were carried out at ISIS Neutron Spallation Source, Rutherford Appleton Laboratory (UK) using the GEM diffraction station. A total of 50 mg of the pure Mo_2N sample, that was obtained by subjecting the commercial material to high P–T treatment, was loaded into a 3-mm-diameter vanadium canister mounted in the sample chamber, that was then evacuated to 10^{-4} mbar. The pattern was collected using the 90° detector with a TOF range of 2–16 ms. Data were collected for 1 h at room temperature. The raw data were summed and the sample chamber contribution to the background removed using in-house (RAL) software. Rietveld analysis was then carried out using the GSAS suite of programmes [15]. The profile coefficients were obtained from the instrument parameter file produced at RAL: it consisted of a convolution of Ikeda-Carpenter (to allow for moderator pulse shape) and pseudo-Voigt functions. The background consisted of an 8-parameter power series expression [16]. The refined lattice parameter, thermal parameters and N site occupancy are reported in Table 1, and the results of the neutron refinement are shown in Fig. 1(b). The thermal parameters and site occupancies for the nitrogen sites are highly correlated, however, by initially allowing only the thermal parameters to be refined to convergence and then both the site occupancies and thermal parameters to be refined it is hoped that the correlations would be minimised.

Table 1
Results of Rietveld refinement of neutron and X-ray diffraction data for γ-Mo_2N

Parameter	X-ray	Neutron
Space group	$Fm\bar{3}m$	$Fm\bar{3}m$
Temperature (K)	290	290
a (Å)	4.1613(1)	4.16158(5)
Volume (Å^3)	72.059	72.073
Mo (4*a*)		
x	0.0	0.0
y	0.0	0.0
z	0.0	0.0
U_{iso} (Å^2)	0.708(14)	0.00666(57)
Site occupancy factor	1.0	1.0
N (4*b*)		
x	0.5	0.5
y	0.5	0.5
z	0.5	0.5
U_{iso} (Å^2)	0.32(24)	0.00547(72)
Site occupancy factor	0.46(1)	0.506(3)
R_p%	9.98	7.7
wR_p%	5.45	4.7
χ^2	3.35	1.39

For in situ high-pressure X-ray diffraction measurements to determine the compressibility, powdered samples of γ-MoN_x samples were loaded into a cylindrical diamond anvil cell. The sample was contained within a 130-μm hole drilled in a Re gasket. Samples were cryogenically loaded with N_2 or Ar as a pressure medium, and ruby chips were added for P-determination Angular-dispersive diffraction studies were performed to 47 GPa at the the UK SRS facility, station 9.1, (Daresbury, UK) with $\lambda = 0.04654$ nm and an image plate detector. Additional measurements were also carried out over a similar pressure range (to $P = 54$ GPa) at the Advanced Photon Source (APS, Argonne National Laboratory, IL, USA), at the GSE-CARS beamline (ID-13 [12]). The sample-to-detector

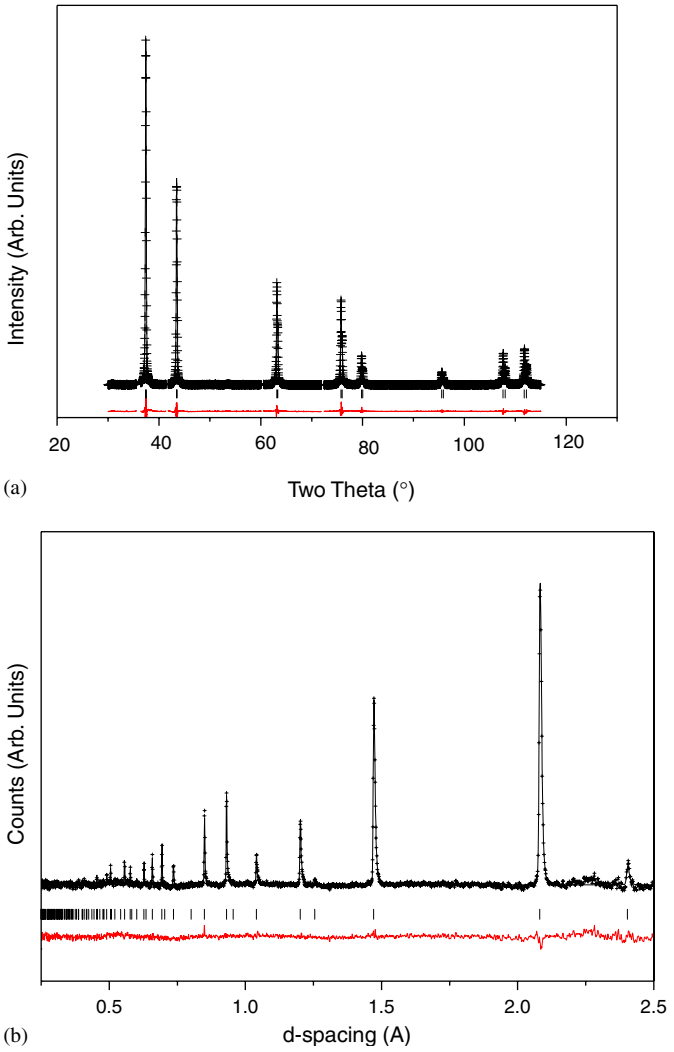

Fig. 1. (a) X-ray diffraction pattern of γ-Mo_2N (observed (+), calculated (−) and difference profile (bottom trace)). (b) The neutron observed (+), calculated (−) and difference profiles (bottom trace) for γ-MoN at 290 K.

distance and the image plate inclination angles were calibrated using a crystalline Si standard. The two-dimensional diffraction images were integrated using OEDIPUS or Fit2D software, yielding one-dimensional intensity vs. diffraction angle (2θ) patterns [17].

DC susceptibility data were collected using a SQUID magnetometer (Quantum design, MPMS) at a magnetic field of 10 Oe over the temperature range 1.8–15 K using field cooling (FC) and zero field cooling (ZFC) processes. The superconducting volume fraction of the sample was estimated from the Meissner behaviour. The Meissner effect of the sample investigated here was weak, and the superconducting volume fraction was estimated at ~5%. Although this is not large, it is sufficient to explain the observed bulk superconductivity. The superconducting volume fraction can vary widely, depending on the microscopic nature of the sample. Raman spectra were obtained out using a home-built high-throughput optical system based on Kaiser® supernotch filters, an Acton® spectrograph system, and a LN_2-cooled back-thinned CCD detector [18]. Spectra were excited using either the 514.5-nm line of an Ar^+ laser or the 633-nm line of a He–Ne laser, focused onto the sample via a 50 × -long working distance Mitutoyo® objective. Raman scattering was collected at 180° geometry through the same lens. Care was taken to maintain the laser power at minimal values (~1 mW), to avoid oxidation of the sample caused by surface heating.

3. Results and discussion

High-pressure–high-temperature treatment of commercially available material resulted in a well-crystallised powdered sample of cubic γ-MoN_x (Fig. 1a). Rietveld refinement of the X-ray data within the $Fm\bar{3}m$ space group of the $B1$-structured nitride yielded a successful fit with $wR_p = 5.45\%$ and $R_p = 9.98\%$ (Table 1, Fig. 1). The TOF neutron diffraction data were also successfully refined within the same space group, giving $wR_p = 4.7\%$ and $R_p = 7.7\%$, and a refined N site occupancy of 0.506(3) (Table 1, Fig. 1b). The lattice parameters determined from neutron and X-ray results were in excellent agreement with each other: $a_0 = 4.16158(5)$ and 4.1613(1) Å, respectively. The concordance between the neutron and the X-ray data, and the successful Rietveld refinements of the powder data within the structural model confirms that all N atoms are confined to octahedral sites within the structure. When using a model in which the nitrogen atoms occupied the tetrahedral sites, no reasonable fit to the data was obtained and therefore confirms the occupation of the octahedral sites. The composition of the material has been determined from the structural refinements and is close to that determined by chemical analyses in previous studies ($Mo_2N \equiv MoN_{0.5}$) [1,4]. The SQUID magnetometry results indicate that a superconducting transition occurs for this $B1$-structured material at $T_c = 5.2$ K (Fig. 2). This value is

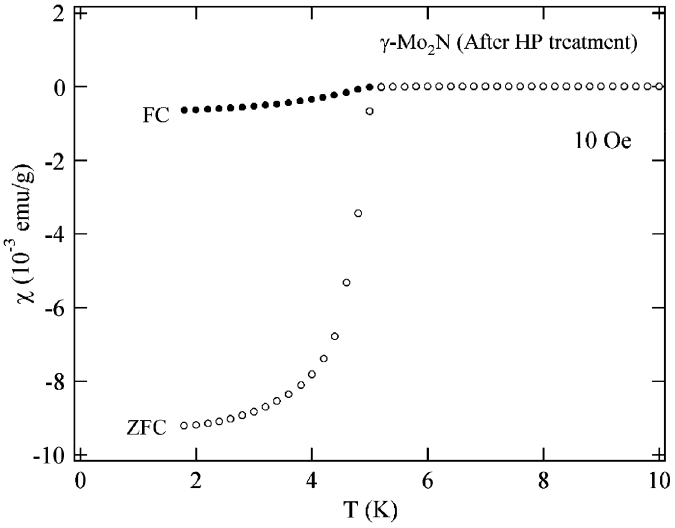

Fig. 2. The SQUID magnetometer results from 1.8 to 10 K.

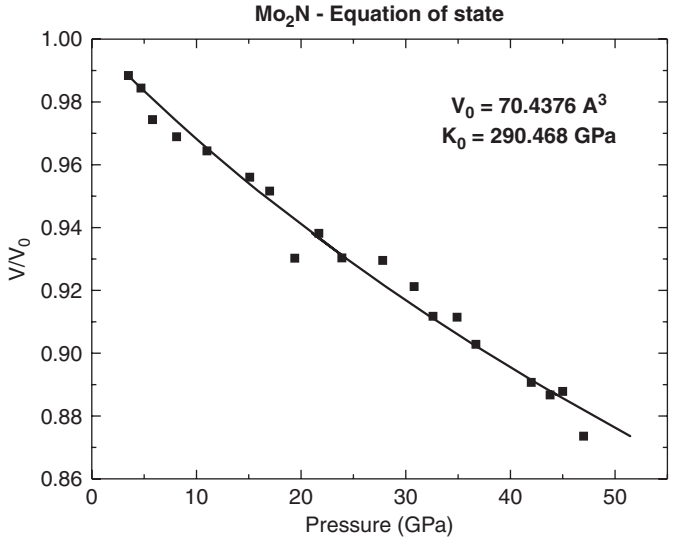

Fig. 3. Plot of V/V_0 for the g-Mo_2N sample as a function of pressure with the fit of the Birch-Murnaghan equation of state (see text for details).

substantially lower than that predicted for the hypothetical mononitride phase (γ-MoN), or those observed for either the ordered or disordered varieties of hexagonal δ-MoN [7,9]. The average Mo–N distance indicated from the structure refinement is 2.081(1) Å, shorter than the values obtained for the hexagonal δ-MoN structure (2.159–2.206 Å). However, the separation between Mo atoms is 2.943 Å, that is comparable with the Mo⋯Mo distances recorded for the hexagonal phase (2.809–3.066 Å) [9]. In these high-density transition nitride metallic structures, it is often considered that the metal atoms engage in metallic bonding, and that the interstitial non-metal atoms simply donate electrons into the valence or conduction bands [1,2]. Our structural results support that view.

Because transition metal nitrides are known to be high-hardness materials, it was of interest to determine the compressibility of Mo_2N in this study. X-ray diffraction patterns were obtained using angle-dispersive synchrotron diffraction at up to $P = 47$ GPa in a diamond anvil cell at SRS (Fig. 3). Complementary data were obtained later at the APS [12], and the results are reported together here. The $V(P)$ data were fitted to a third-order Birch-Murnaghan equation of state [19–21]:

$$P(V) = 3K_0 f(1+2f)^{5/2}\left(1+\frac{3}{4}(K_0'-4)f\right) \quad (1)$$

in which the Eulerian strain variable (f) is expressed as

$$f = \frac{1}{2}\left[\left(\frac{V}{V_0}\right)^{-2/3} - 1\right]. \quad (2)$$

In order to determine the compressibility parameters, K_0' was initially set to 4 to obtain a first estimate of V_0 and K_0. Then a plot of f vs. the normalised pressure (F):

$$F = P[3f(1+2f)^{2.5}]^{-1} \quad (3)$$

was used to determine best fit values for all parameters. The fitted value of the V_0 parameter was 70.44 Å^3, close to the experimentally determined value at ambient conditions: (72.04 Å^3: Table 1). The refined values of K_0 and K_0 were 304(1) and 4.0(2) GPa, respectively [12]. The bulk modulus is identical with a value previously estimated for a nanocrystalline sample prepared by chemical metathesis synthesis [6].

Although elevated values of the bulk modulus is not always an indication of high hardness among materials in general, the relation between hardness and K_0 applies quite well among the high-symmetry refractory transition metal carbides and nitrides [22,23]. The technologically important cubic phase TiN has $K_0 = 290$ GPa and a Vickers hardness of 2100 kg/mm^2, WC achieves $K_0 \approx 421$ GPa and $V_H = 2400$ kg/mm^2, and hexagonal δ-MoN reaches $K_0 =$ 345 GPa [3,6]. The bulk modulus is correlated with the cohesive energy per unit molar volume (E_c/V_m), that constitutes a primary factor determining hardness; an empirical relationship relating these parameters is

$$K_0 = c\frac{E_c}{V_m}. \quad (4)$$

In this equation, c is an empirical constant, $c = 2-4$ [24]. The values of E_c/V_m and K_0 can be correlated using simple electron-counting techniques to determine the distribution of electrons between bonding and anti-bonding levels [1–3]. Within cubic nitride structures, TiN has $(4+5)/2 = 4.5$ valence electrons, and Mo_2N has $(6 \times 2.5)/2 = 4.25$ valence electrons. We thus expect that Mo_2N should have greater cohesive energy than TiN, because the anti-bonding levels

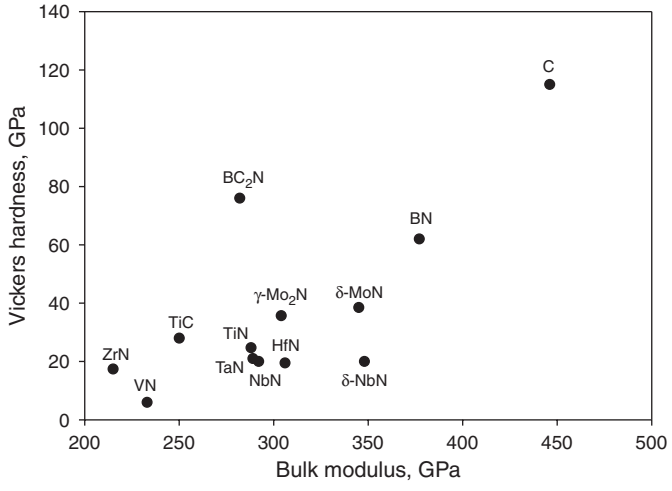

Fig. 4. Relation of bulk modulus and Vickers hardness for selected materials. Data on bulk moduli are taken: for C diamond from Gillet et al. [25]; for BN from Solozhenko et al. [26]; for δ-NbN, NbN, HfN and ZrN from Chen et al. [27]; for TiN from Shebanova et al. [28]; for TaN from Soignard et al. [29]; for BC_2N from Solozhenko et al. [30]; for TiC from Jhi and Ihm, [31]; for VN from Zhukov et al. [32]; for γ-Mo_2N and δ-MoN from Soignard et al. [33]. Data on Vickers hardness are taken: for C (diamond), BN and BC_2N from Solozhenko et al. [30]; for δ-NbN, NbN, HfN and ZrN from Chen et al. [27]; for TiN, TaN and TiC from Musil, [34]; for VN from Davies et al. [35]; for γ-Mo_2N and δ-MoN from Ürgen et al. [36].

have started to fill within TiN compounds, whereas the Fermi level within Mo_2N is at a lower energy than the anti-bonding states [1–3]. This analysis is combined with our present measurement of the bulk modulus of γ-Mo_2N to predict that Mo_2N should be a higher hardness phase than TiN (Fig. 4).

It has been shown for cubic nitride materials (TiN_x) that the superconducting transition can be related to lattice dynamic instabilities in the shear acoustic modes at the Brillouin zone boundary, that can be correlated with features observed in the Raman spectra of non-stoichiometric materials [25,27]. These $B1$-structured materials normally have no first-order Raman spectra allowed by symmetry. However, vacancies on the anion sites in TiN_x or γ-Mo_2N leads to relaxation of the selection rules, and the Raman spectra contain broad bands that reflect the vDOS of these materials. The observed features include Ti–N/Mo–N stretching modes at high frequency, and low-wavenumber bands that are due to the acoustic (longitudinal (LA) and transverse (TA)) branches. Following Spengler et al. [37] and Chen et al. [27], we should be able to correlate the positions of the TA modes of NbN and γ-Mo_2N $B1$-structured nitrides with their T_c values. The Raman spectrum of γ-Mo_2N (Fig. 5a) recorded here is analogous to the v-DOS spectrum obtained for the high-T_c superconductor NbN, determined by inelastic neutron scattering [38] (Fig. 5b). However, the superconducting T_c of γ-Mo_2N is only ~5 K, compared with $T_c = 17$ K for cubic NbN [1]. We conclude that the lowered value of T_c for the γ-Mo_2N phase compared to NbN must be due to differences in the electronic occupancy in the vicinity of the Fermi level for these isostructural $B1$-cubic materials.

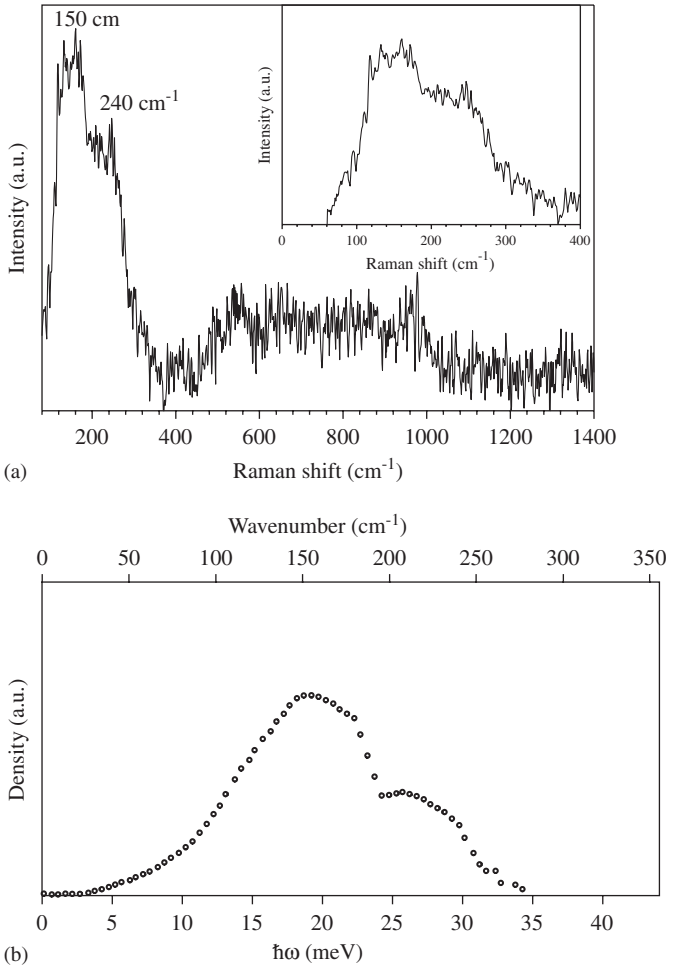

Fig. 5. (a) Raman spectrum of γ-Mo_2N nitride. The broad feature between 500 and 1000 cm^{-1} is a combination of the second-order acoustic modes and the first-order optical modes. (b) Phonon density of states for γ-NbN obtained via inelastic neutron scattering [25].

4. Conclusions

We used high-P,T methods to prepare an ordered cubic γ-$MoN_{0.5}$ (Mo_2N) sample with the rock-salt ($B1$) structure, containing ~50% vacancies on the anion (N^{3-}) sites. The atom site occupancies were determined by Rietveld refinement of a combination of TOF neutron diffraction data and X-ray diffraction results. The results showed that N atoms occupy only octahedral sites within the structure. The disordered cubic γ-Mo_2N material is superconducting, with $T_c = 5.2$ K. It is also a low-compressibility, potentially high-hardness material, with a high value of the bulk modulus $K_0 = 304$ GPa. The Raman spectrum measured for the γ-Mo_2N phase is similar to that of cubic $B1$-structured NbN, that is a superconductor with a much higher value of T_c (17 K). A first-order Raman spectrum is present for γ-Mo_2N due to N^{3-} vacancies appearing within the $B1$-cubic nitride structure, so that the TA acoustic modes associated with a shear instability leading to superconductivity in these materials could be observed. The lowered T_c of Mo_2N vs. NbN is likely due to differences in the electron-filling scheme among states near the Fermi level in the two phases.

Acknowledgments

TK thanks NIMS for an international post-doctoral fellowship. PFM is a Wolfson-Royal Society Research Merit Award fellow, and was supported by EPSRC Grant GR/R65206 for this study. CLB is supported by an EPSRC post-doctoral fellowship to R.J. Nelmes (University of Edinburgh). The authors thank CCLRC for providing direct access to the ISIS facility.

References

[1] L.E. Toth, Transition Metal Carbides and Nitrides, Academic Press, New York, London, 1971.
[2] S.T. Oyama, The Chemistry of Transition Metal Carbides and Nitrides, Blackie Academic and Professional, Glasgow, 1996.
[3] R. Riedel (Ed.), Handbook of Ceramic Hard Materials, vols. 1 and 2, Wiley-VCH, Weinheim, 2000.
[4] G. Hägg, Z. Phys. Chem. B 7 (1930) 339–362.
[5] J.K. Hulm, M.S. Walker, N. Pessall, Physica 55 (1971) 60–68.

[6] E. Soignard, P.F. McMillan, T.D. Chaplin, et al., Phys. Rev. B 68 (2003) 132101–132104.
[7] A. Bezinge, K. Yvon, J. Muller, W. Lengauer, P. Ettmayer, Sol. State Commun. 63 (2) (1987) 141–145.
[8] W.J. Lengauer, J. Cryst. Growth 87 (1988) 295–298.
[9] C.L. Bull, P.F. McMillan, E. Soignard, K. Leinenweber, J. Solid State Chem. 177 (2004) 1488–1492.
[10] D.A. Papaconstantopolos, W.E. Pickett, B.M. Klein, L.L. Boyer, Phys. Rev. B 31 (1984) 752.
[11] G.L.W. Hart, B.M. Klein, Phys. Rev. B 61 (2000) 3151.
[12] D. Machon, D. Daisenberger, E. Soignard, et al., Phys. Status Solidi, submitted.
[13] W.G. Williams, R.M. Ibberson, P. Day, J.E. Enderby, Physica B 241–243 (1998) 234–236.
[14] F. Izumi, T. Ikeda, Mater. Sci. Forum 198 (2000) 321–324.
[15] A.G Larson, R. von Dreele, GSAS manual, Los Alamos Report No LA-UR-86-748 (1987)
[16] W.I.F. David, J. Appl. Crystallogr. 19 (1986) 63–64.
[17] A.P. Hammersley, S.O. Svensson, M. Hanfland, et al., High Pressure Res. 14 (1996) 235.
[18] E. Soignard, P.F. McMillan, Chem. Mater. 16 (2004) 5344–5349.
[19] F.D. Murnaghan, Proc. Nat. Acad. Sci. 30 (1944) 244.
[20] F. Birch, J. Geophys. Res. 37 (1952) 227.
[21] F. Birch, J. Geophys. Res. 83 (1978) 1257.
[22] D.M. Teter, Mater. Res. Sci. Bull. 23 (1998) 22.
[23] P.F. McMillan, Nat. Mater. 1 (2002) 19–25.
[24] V.V. Brazhkin, A.G. Lyapin, R.J. Hemley, Phil. Mag. A 82 (2002) 231.
[25] Ph. Gillet, G. Fiquet, I. Daniel, B. Reynard, Phys. Rev. B 60 (1999) 14660–14664.
[26] V.L. Solozhenko, D. Häusermann, M. Mezouar, M. Kunz, Appl. Phys. Lett. 72 (1998) 1691–1693.
[27] X.-J. Chen, V.V. Struzhkin, Z. Wu, M. Somayazulu, J. Qian, S. Kung, A.N. Christensen, Y. Zhao, R.E. Cohen, H.-K. Mao, R.J. Hemley, Appl. Phys. Sci. 102 (2005) 3198–3201.
[28] O. Shebanova, E. Soignard, P.F. McMillan. Compressibilities and phonon spectra of cubic TiN_x and γ-$MoN_{0.5}$ at high pressure, to be published.
[29] E. Soignard, O. Shebanova, P.F. McMillan, Phonon spectra and compressibilities of hexagonal transition metal nitrides at high pressure, to be published.
[30] V. Solozhenko, D. Andrault, G. Fiquet, M. Mezouar, D.C. Rubie, Appl. Phys. Lett. 78 (2001) 1385–1387.
[31] S.H. Jhi, J. Ihm, Phys. Rev. B 56 (1997) 13826–13829.
[32] V.P. Zhukov, V.A. Gubanov, O. Jepsen, N.E. Christensen, O.K. Andersen, J. Phys. Chem. Solids 49 (1988) 841.
[33] E. Soignard, P.F. McMillan, T.D. Chaplin, S.M. Farag, C.L. Bull, M.S. Somayazulu, K. Leinenweber, Phys. Rev. B 68 (2003) 132101-1-132101-4.
[34] J. Musil, Surf. Coat. Technol. 125 (2000) 322–330.
[35] K.E. Davies, B.K. Gan, D.R. McKenzie, M.M.M. Bilek, M.B. Taylor, D.G. McCulloch, B.A. Latella, J. Phys: Condens. Matter 16 (2004) 7947–7954.
[36] M. Ürgen, O.L. Eryilmaz, A.F. Çakir, E.S. Kayali, B. Nilüfer, Y. Işik, Surf. Coat. Technol. 94–95 (1997) 501–506.
[37] W. Spengler, R. Kaiser, A.N. Christensen, G. Muller-Vogt, Phys. Rev. B 17 (1978) 1093–1101.
[38] H. Bilz, W. Kress, Phonon Dispersion Relations in Insulators, vol. 10, Springer, Berlin, Heidelberg, New York, 1979.